C ec i n f m a i n i hin he c ic fib i an memb ane c nd c ance eg la b i e-di ec ed RNA edi ing

M F M -G ', H1 V -V ', G A. Y 1 ', J 1 J. C. R 1 ', 1

a

λ-phage RNA-binding protein, ADAR's deaminase domain can be coupled to an antisense RNA oligonucleotide inside a cell and that the complex can guide site-specific mRNA editing and correct premature termination.

[illegible]. Our overall strategy for generating a site-directed editase was to link human ADAR2's deaminase domain to an antisense guide oligonucleotide through an interaction that could be genetically encoded. With this in mind, we looked for an RNA-binding protein that recognizes a specifi

channels were obvious candidates. We selected the W496X mutation in the cystic fibrosis transmembrane conductance regulator (CFTR) for several reasons (24). As with many other mutations in CFTR, W496X leads to terminal cystic fibrosis, the most common genetic disease in whites. CFTR itself is an anion channel that is expressed in a variety of epithelial cells, including those within the lung. When activated by ATP and cAMP, a single CFTR channel creates a conductance of ~7–10 pS (25). Because codon 496 is located only a third of the way through the ORF, a premature termination would create a no3(mincr8d13.2(cre)17.nufcre)17.nufcree ease

As a final indication of correction, we tested whether functional CFTR-mediated currents had been restored (Fig. 4). CFTR channels require ATP and cAMP to open. In oocytes, resting ATP levels are sufficient (29, 30); however, cAMP levels need to increase, and experimentally this can be accomplished by adding extracellular forskolin to stimulate adenylyl cylase activity. Fig. 4*B* shows an example of a "chart" record of membrane currents from a complete experiment recorded on a slow-time base. In this case, the oocyte was injected with wild-type CFTR, but the same approach was used for all recordings. Oocytes were held at −40 mV. At this voltage with our external solution, chloride ions will leave the cell through open CFTR channels, creating an apparent inward current. At various times during the procedure, we stepped the voltage from −80 to +40 mV in 20-mV increments (I–V) and recorded the resulting currents. These I–Vs are seen as rapid vertical deflections, and the two that we used for analysis have been labeled (1, 2). After two I–Vs, external forskolin was added, causing an inward current to develop. In Fig. 4*C* we show I–Vs before and after forskolin, recorded on a rapid-time base. Here, with wild-type CFTR, robust currents of greater than 10 μA are activated. When the same experiment was performed on oocytes injected with CFTR W496X, no currents were activated. However, when oocytes were injected with λN–DD36p(DD)-DD

N

(RNA Polymerase III) promoter. This guide was able to direct 92 ± 1.2% editing (n = 3) at W58X in vitro as assessed by RT-PCR. As expected, wild-type EGFP-transfected HEK-293T cells gave a strong fluorescence signal, and EGFP W58X gave no detectable signal (Fig. 5*A*). EGFP W58X controls that lacked either λN–DD or the guide also yielded no detectable signal. In contrast, when EGFP W58X was transfected with both λN–DD and the guide, a strong signal was evident in many cells. A quantification of the fluorescence from individual cells revealed that the relative intensity of experimental cells was about 12% that of wild-type EGFP (see legend for Fig. 5). Direct sequences of the entire EGFP W58X cDNA revealed that ~20% of the premature termination codon had been corrected in experimental plates (Fig. 5*B*). Moderate off-target editing was encountered at Y146S (9 ± 5.4%; n = 3) and K167R (38 ± 6.1%; n = 3). From these results we conclude that we can use genetically encoded λN–DD and guide RNA to restore function in a human cell.

Discussion

The correction of genetic mutations in mRNA is attractive for several reasons. First, compared with DNA, mRNA is accessible. Genomic DNA is sequestered in the nucleus and often tightly bound by histones. Mature mRNA, on the other hand, is in the cytoplasm. Furthermore, RNA cannot integrate into the genome and is relatively unstable, making off-target edits less of a concern than with approaches that target DNA. Another advantage for site-directed RNA editing is that it should not affect mRNA expression level. For many proteins, the precise level of expression is critical as both underexpression and overexpression can lead to disease. The MeCP2 protein is a good example where underexpression leads to Rett syndrome, and even mild overexpression can lead to autism spectrum disorders (31). Finally, many potential tools are available for RNA manipulation because there are several enzymes that can modify RNA in a base-specific manner.

To date, there have been few reports of site-directed RNA editing. Most have sought to induce endogenously expressed enzymes to correct a specific mutation by introducing a guide RNA. For example, many cellular RNAs contain pseudouridine, a *c*-glycoside isomer of the nucleoside uridine created by pseudouridine synthase. In tRNAs, specific uridines are marked for pseudouridylation by an appropriate guide RNA. When pseudouridines are present within mRNAs, they can recode a codon (32). For example, the pseudouridylated stop codons UAA and UAG are read as either serine or threonine, and UGA is read as tyrosine or phenylalanine. Targeting pseudouridylation to a premature termination codon in yeast induces read-through. A similar, albeit less specific, approach was used with endogenous ADARs. When presented with a perfect RNA duplex, ADARs will edit promiscuously. By introducing RNA oligonucleotides complementary to a premature termination codon, Woolf et al. induced endogenous ADAR to nonspecifically edit the region, including the premature termination codon, both in vitro and in *Xenopus* embryos (33). A recent study has reported a more directed approach, similar to our own (34). In it the authors coupled the catalytic domain of human ADAR1 to a guide RNA oligonucleotide using an in vitro reaction. Using this hybrid enzyme, a premature termination codon introduced into a fluores-

oligonabl.9(8itro)5(a)8uide8 89ide 8 fi

. See *SI Methods* and Table S1.

. Before the editing assay, the antisense RNA oligonucleotide or guide RNA was annealed to the RNA target using a ramp from 65 °C to 25 °C, decreasing –1 °C every 15 s. Editing assays were performed at 25 °C for 2 h with 4boxB mRNA or at 35 °C for 2 h with SqKv1.2 or CFTR mRNAs. For the data presented in Fig. 1, the assay contained 2.5 nM 4boxB RNA, 75 nM recombinant λN–DD, 2.5 nM antisense oligonucleotide, 5 mM DTT, 5 mM PMSF, 0.5 μg/μL tRNA, and 1 U/μL murine RNase inhibitor, all in Q75 [50 mM, Tris pH 7.9, 75 mM potassium chloride, and 10%(wt/vol) glycerol]. All other assays contained 2.25 nM target RNA, 75 nM recombinant λN–DD, 20 nM guide RNA oligonucleotide, 5 mM DTT, 5 mM PMSF, 0.5 μg/μL tRNA, and 1 U/μL murine RNase inhibitor, all in Q200 (same as Q75 except 200 mM potassium glutamate was substituted for the 75 mM potassium chloride). For blocking control assays, we added 7.5 μM boxB or boxB mutant oligonucleotide or 250 μM λN peptide. λN peptide was purchased from New England Peptide. BoxB and mutated boxB RNAs (G8A, A10C) were synthesized commercially.

. After editing in vitro, cDNA was synthesized using the AccuScript High-Fidelity RT-PCR Kit (Agilent Technologies). After amplifying the cDNA by PCR, products were sent for direct sequencing. Quantification of editing percentages was performed by comparing the deoxycytidine/deoxythymidine peak heights in the antisense strand according to published protocols (37, 38).

Xenopus **.** On day 1, oocytes were injected with 368 fmol of λN–DD. After 3 d, they were reinjected with 1 pmol (electrophysiology)

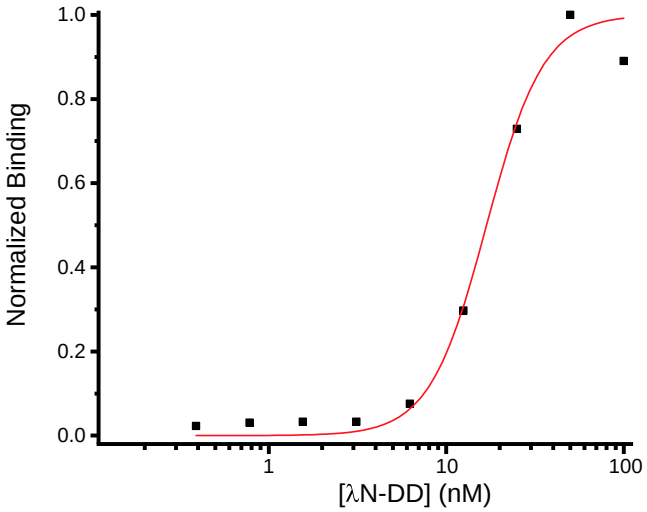

F . S1. Recombinant λN-DD binds boxB RNA. To determine the binding affinity between λN-DD and the boxB guide RNA, we performed filter binding assays (1). We transcribed guide RNA SqKv1.2 with T7 RNA polymerase in the presence of 35 μCi of [α-^{32}P]UTP (3,000 Ci/mmol; 1 Ci = 37 GBq), 1X T7 buffer, rCGU mix (3.3 mM final concentration each), 2 mM rA, 0.1 M DTT, RNase Inhibitor. The binding reaction contained Q200 potassium glutamate (K-Glu) buffer, pH 7 [200 mM K-Glu, 10 mM Tris glutamate, pH 7, and 20% (wt/vol) glycerol]; in addition, we added 1 mM DTT, 0.5 mM PMSF, 0.5 μg/μL tRNA, and 1 U/μL RNase inhibitor in a volume of 30 μL. The reaction was incubated at 37 °C for different times (5, 10, 15, 30, 60, 120, and 180 min) to determine the time when the reaction reached equilibrium. Binding assays were performed by adding 5,000 cpm of guide RNA and different dilutions of λN-DD (100, 50, 25, 12.5, 6.25, 3.125, 1.56, 0.78, 0.39, 0.19, 0.09, 0.04, and 0.02 nM). To determine the K_d, fraction-bound RNA was plotted versus different concentrations of λN-DD and fit the graph to a Boltzmann function of the formula $F = [\lambda N - DD]$

T S1. DNA RNA 1 1 1

Oligonucleotide no.	Oligonucleotide name	Sequence	Target sequence	Associated text figure	Description
1	MF1	AGACTAGTAAACGCACGAACACGACGACGT	1–21 λ		

T S1. C .

Oligonucleotide no.	Oligonucleotide name	Sequence	Target sequence	Associated text figure	Description
18	Guide DNA C (AS)	5′GGGTGGAAGAATTTGGCCTTTTTCAGGGCCTCTGTTCTCAGTTT TCCTAGATTTCTCCCTA TAGTGAGTCGTATTA3′	1452–1465 and 1469–1491 CFTR	Figs. 2, 3, and 4	Antisense DNA oligonucleotide used to synthesize guide C RNA for CFTR W496X in vitro editing assay; has 5′ T7 tag
19	BoxB RT	GGCGTACAGGGACAGAACAGCTTGGGGCAGAATCCAGATGCTC	302–319 4boxB	Fig. 1	RT primer for making 4boxB cDNA; contains a 5′ ACT2 (primer 24) tag
20	BoxB1	TAAGCTCGCTTTCTTGCTGTCC	1–22 4boxB	Fig. 1	Fwd PCR primer to amplify 4boxB cDNA
21	BoxB2	ATTAGGCAGAATCCAGATGCTC	302		